NURETH14-016

A NOVEL INFRARED-BASED EXPERIMENTAL TECHNIQUE TO DETECT PHASE DYNAMICS ON BOILING SURFACES

H. D. Kim^{1,2}, Jacopo Buongiorno¹

¹ Massachusetts Institute of Technology, Cambridge, Massachusetts, USA
² Kyung Hee University, Youngin, Gyeonggi 446-701, Republic of Korea, hdkims@khu.ac.kr, jacopo@mit.edu

Abstract

Heat transfer in nucleate boiling is strongly affected by the liquid and vapor phase distribution on the boiling surface. A novel experimental technique for the detection of phases on boiling surfaces is presented. The technique is based on high-speed infrared (IR) thermometry through an IR-transparent silicon wafer heater; hence the name DEPIcT, or DEtection of Phase by Infrared Thermometry. Where the heater surface is wet, the IR camera measures the temperature of the hot water in contact with the heater. On the other hand, where vapor (whose IR absorptivity is very low) is in contact with the heater, the IR light comes from the cooler water beyond the vapor. The resulting IR image appears dark (cold) in dry spots and bright (hot) in wetted area. Using the contrast between the dark and bright areas, we can visualize the distribution of the liquid and gas phases in contact with the heater surface, and thus identify also the liquid-vapor-solid contact line. DEPIcT is able to detect thin liquid layers, through the analysis of interference patterns. Finally, the technique is applied to nucleate boiling of water at atmospheric pressure to gain insight into the surface micro-hydrodynamics at high heat fluxes, all the way up to CHF.

Keywords: micro-hydrodynamics, CHF, DEPIcT

1. Introduction

Complex two-phase heat transfer phenomena such as nucleate boiling, critical heat flux, quenching and condensation govern the thermal performance of Light Water Reactors (LWRs) under normal operation and during transients/accidents. These phenomena are typically characterized by the presence of a liquid-vapor-solid contact line on the surface from/to which the heat is transferred. For example, in nucleate boiling, a significant fraction of the energy needed for bubble growth comes from evaporation of a liquid meniscus, or microlayer, underneath the bubble itself, as shown in Fig. 1a. As the liquid-vapor-solid line at the edge of the meniscus retreats, a circular dry patch in the middle of the bubble is exposed; the speed of the triple line retreat is a measure of the ability of the surface to transfer heat to the bubble. At very high heat fluxes, near the upper limit of the nucleate boiling regime, also known as Critical Heat Flux (CHF), the situation is characterized by larger dry areas on the surface, dispersed within an interconnected network of liquid menisci (see Fig. 1b). In quenching heat transfer, which refers to the rapid cooling of a very hot object by immersion in a cooler liquid, the process is initially dominated by film boiling. In film boiling a continuous vapor film completely

separates the liquid phase from the solid surface; however, as the temperature gets closer to the Leidenfrost point, intermittent and short-lived liquid-solid contacts occur at discrete locations on the surface, thus creating liquid-vapor-solid interfaces once again (see Fig. 1c). Ultimately, if bubble nucleation ensues at such contact points, the vapor film is disrupted and the heat transfer regime transitions from film boiling to transition boiling. Finally, in dropwise condensation, the phase transition from vapor to liquid occurs via formation of discrete droplets on the surface (see Fig. 1d), and the resulting liquid-vapor-solid triple line is where heat transfer is most intense.

To gain insight into and enable mechanistic modeling of all these two-phase heat transfer phenomena, there is clearly a need to detect the liquid-vapor-solid triple contact line and measure its physical characteristics (extension, speed, temperature). In this paper we demonstrate the application to boiling heat transfer of a recently-developed experimental technique, named DEPIcT [1]. The technique is briefly described in Section 2, while its use for the more complex situations of nucleate boiling and CHF is discussed in Section 3.

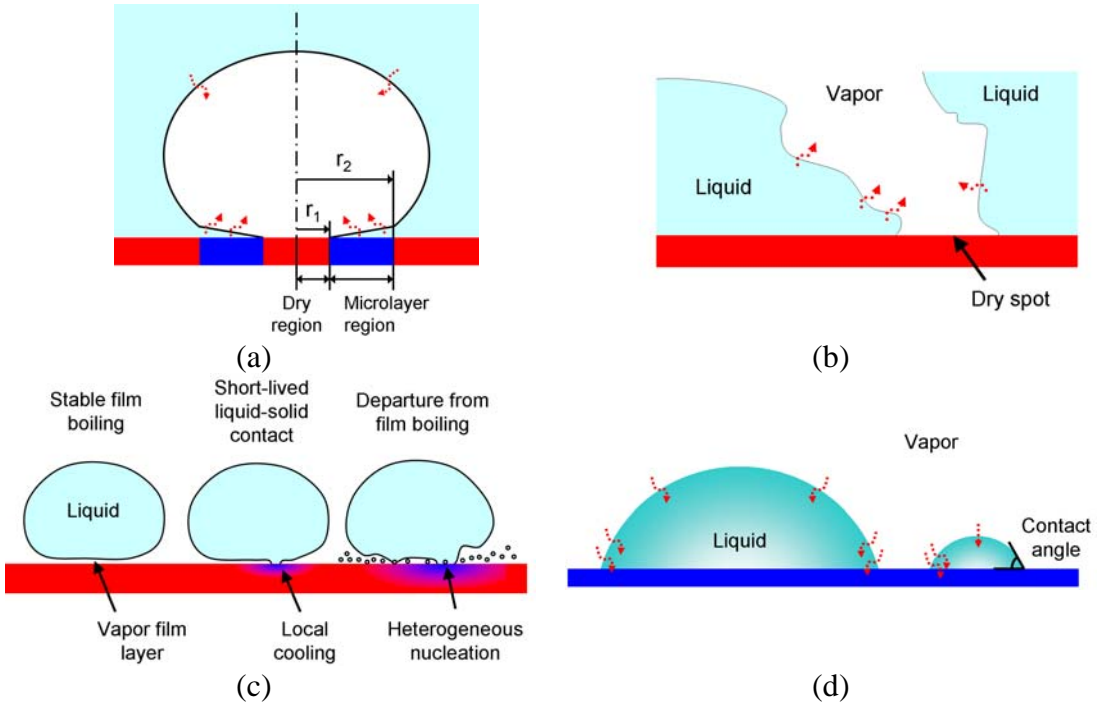


Figure 1. Representation of physical situation for (a) bubble growth, (b) high-heat-flux nucleate boiling, (c) Leidenfrost point, and (d) dropwise condensation.

2. Description of the experimental technique

DEPIcT (DEtection of Phase by Infrared Thermometry) exploits temperature differences to detect the liquid-vapor-solid triple contact line. An IR camera is used to detect the phases present on a heated surface. The key feature of this technique is to use a heater material that is IR transparent (e.g. optical grade silicon wafer), and a fluid that has a very high IR absorptivity (e.g. water). The IR camera is placed below the heater, while the fluid lies on top (Fig. 2). Where the heater surface is wet, the IR camera measures the temperature of the hot water in contact with the heater. On the other hand, where vapor (whose IR absorptivity is very low) is in

contact with the heater, the IR light comes from the cooler water beyond the vapor. The resulting IR image appears dark (cold) in dry spots and bright (hot) in wetted area. Using the contrast between the dark and bright areas, we can visualize the distribution of the liquid and gas phases in contact with the heater surface, and thus identify the liquid-vapor-solid contact line. In other words, we measure temperature *beyond* the surface to detect phases *on* the surface. This approach distinguishes DEPIcT from the now-established IR thermometry technique with IR-opaque heaters [2-4], where the temperature measured is the temperature of the surface, which makes it hard to identify phases on the surface conclusively.

The IR camera used in this study is a SC6000, FLIR Systems Inc., with an IR wavelength range of 3-5 μ m. Optical grade silicon wafer with the following properties was used as the heater: <100> orientation, P/Boron-doped, electrical resistivity 5-25 Ω -cm, thickness 380±25 μ m, and double side polished. The relatively high electrical conductivity of this doped silicon made it possible to use direct (Joule) heating in boiling experiments. The silicon wafer heater is completely opaque to visible light, but transparent to IR. With this setup the liquid-vapor-solid contact line can be detected with a typical accuracy of $\pm 100~\mu$ m. A complete description of DEPIcT, including an assessment of its uncertainties is reported in [1]. Briefly, the IR camera used in this study has a temperature resolution of 0.025°C, a maximum frame rate of 125 fps at full spatial resolution of 640×512 pixels and higher frame rates at a subset of the total image, i.e. 1000 fps at 144×144 pixels. The actual spatial resolution depends obviously on the physical size of the object being imaged. For example, if we are interested in imaging an area of 1 cm² and use 100×100 pixels, the spatial resolution is 100 μ m. This is also the spatial uncertainty with which the contact line can be detected. Other limitations of DEPIcT include the need for an IR-opaque fluid and an IR-transparent substrate.

A simple example of DEPIcT application is shown in Fig. 3.

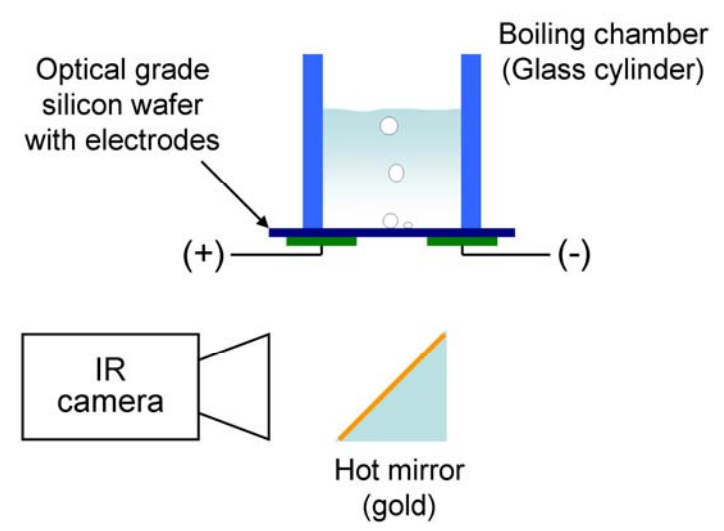


Figure 2. Schematic diagram of the DEPIcT technique. The IR camera takes an image through the wafer.

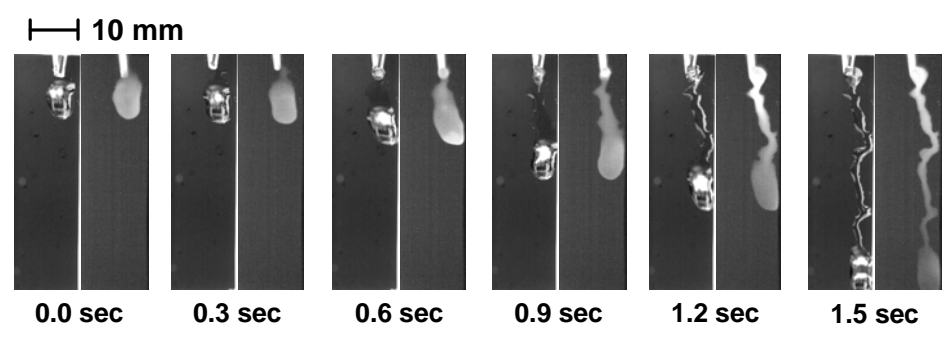


Figure 3. Droplet (~30°C) sliding on a vertical silicon wafer (~24°C). Comparison of the high-speed video (left) and IR (right) images taken from the front and back of the wafer, respectively. The sharpness of the IR image through the wafer confirms that the wafer is transparent to IR.

3. Applications

DEPIcT has been applied to single-bubble growth (Section 3.1), bubble-bubble interaction in low heat-flux nucleate boiling (Section 3.2), and micro-hydrodynamics of liquid menisci in high heat-flux nucleate boiling, including CHF (Section 3.3). In all these boiling experiments the doped silicon wafer was accommodated into a $50\times50~\text{mm}^2$ square silicon substrate with Au/Cr metal pads for electrical connection to a 250-V 30-A DC power supply. The substrate had a $14\times9~\text{mm}^2$ opening at the center to allow for imaging by the IR camera underneath. Boiling occurred on the top face of the heater (Fig. 2). The boiling chamber was a glass cylinder of 50-mm outer diameter and 50-mm length, attached and sealed to the top face of the wafer.

3.1 Nucleation, growth and departure of isolated bubble

We looked at nucleation, growth and departure of a single bubble first. Figure 4 shows the temporally and spatially synchronized images of the High Speed Video (HSV) and IR cameras for the bubble. The IR images show various features of the growing bubble, including a dry (dark) spot at the center of the bubble, and, up to 5 ms, an outer (less dark) rim, which corresponds to the so-called microlayer [5] underneath the bubble, as shown in Fig. 1a. Analysis of the interference rings in the rim enables measurement of the microlayer thickness vs time, as shown in Fig. 5 and explained in detail in Ref. [1]. At ~5 ms the microlayer has completely evaporated. After 5 ms, the triple contact line starts to advance toward the bubble axis, as the bubble is detaching from the surface under the effect of buoyancy. The image at 14 ms shows that only the tiny tail of the bubble is attached to the heater surface.

3.2 Bubble-bubble interaction in nucleate boiling

Interactions of bubbles in nucleate boiling (in the so-called discrete bubble regime) were investigated with DEPIcT, as shown in Fig. 6. Three bubbles, 'A', 'B' and 'C', nucleate at different locations and times. Note that the bubbles display the same physical characteristics of the single bubble in Fig. 4, with an inner dry (dark) spot, surrounded by a microlayer (gray). The first two bubbles, 'A' and 'B', do not interact with each other because of the large spacing between them, ~7.2 mm. On the other hand, the third bubble 'C', which nucleates at 4 ms, is close to bubble 'B', ~3.5 mm. Now, the HSV shows that the 'B' and 'C' merge to form a large mushroom-type bubble, but the IR images clearly show that the *roots* of the bubble do not merge

in the process, i.e., a bright (liquid) filament continues to separate the roots of the two bubbles until the mushroom bubble detaches from the surface at 12 ms. These observations are in agreement with the criterion suggested by Zhang and Shoji [6], according to which for $S/\overline{D}_b > 3$ the hydrodynamic interaction between bubbles is negligible, while for $S/\overline{D}_b \le 1.5$ both hydrodynamic and thermal interactions are very strong. Here S is the spacing between bubbles and \overline{D}_b is the bubble diameter.

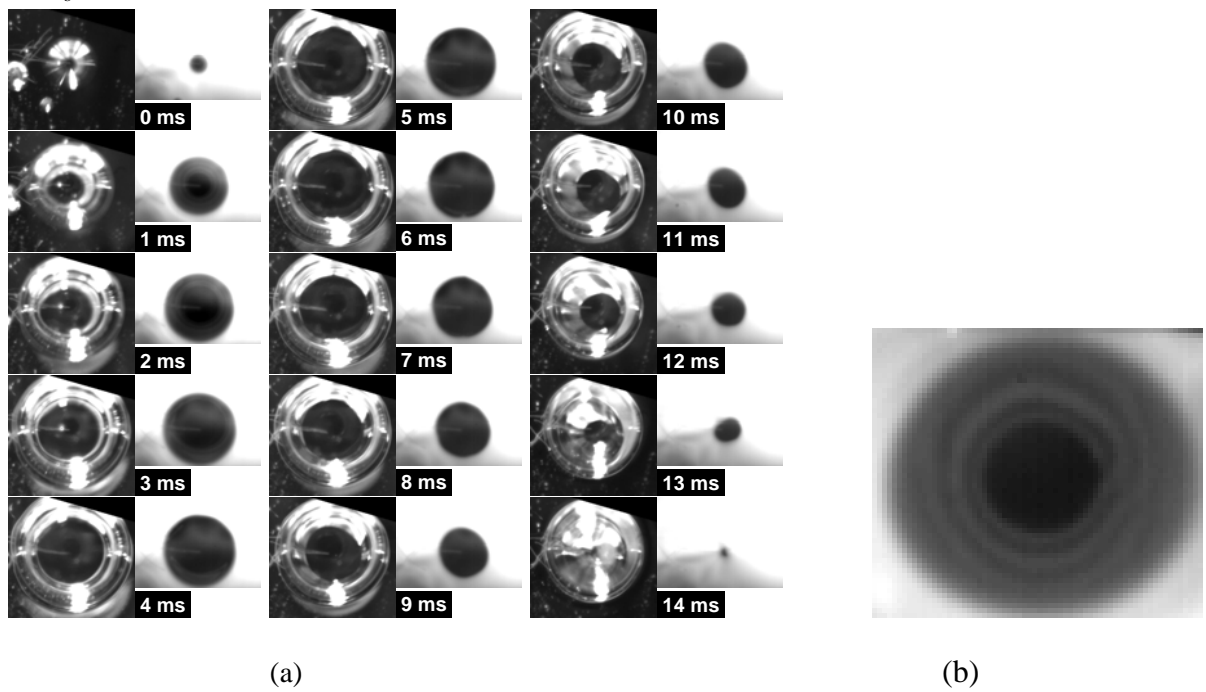


Figure 4. Bubble nucleation, growth and departure in saturated water on an electrically-heated silicon wafer: (a) synchronized HSV and IR pictures. (b) interference rings are clearly visible between the dry center of the bubble base and the outer wet region of the wafer.

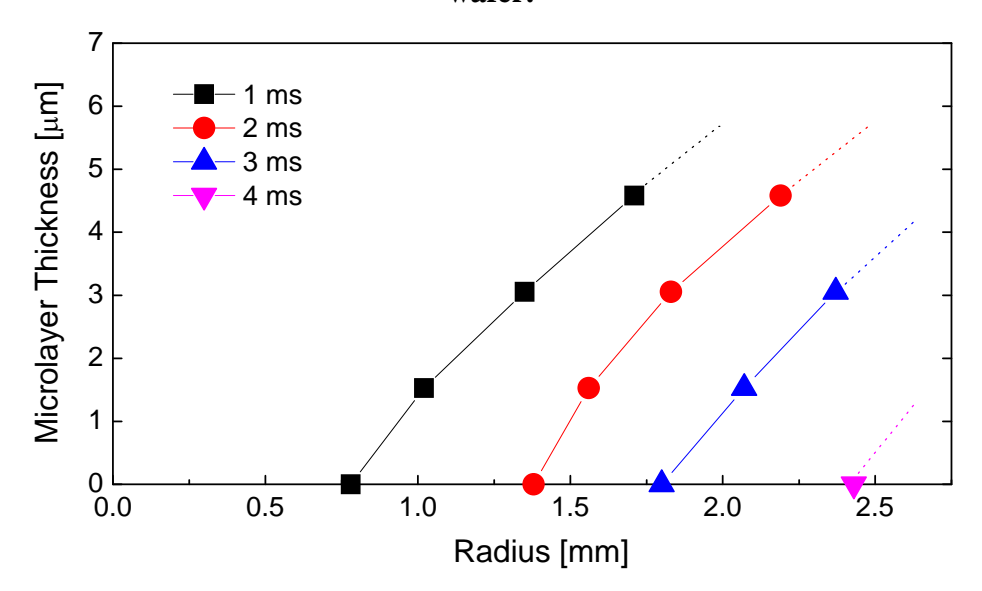


Figure 5. Microlayer shape vs time underneath a growing bubble. "Radius" refers to the radial distance from the center of the bubble root.

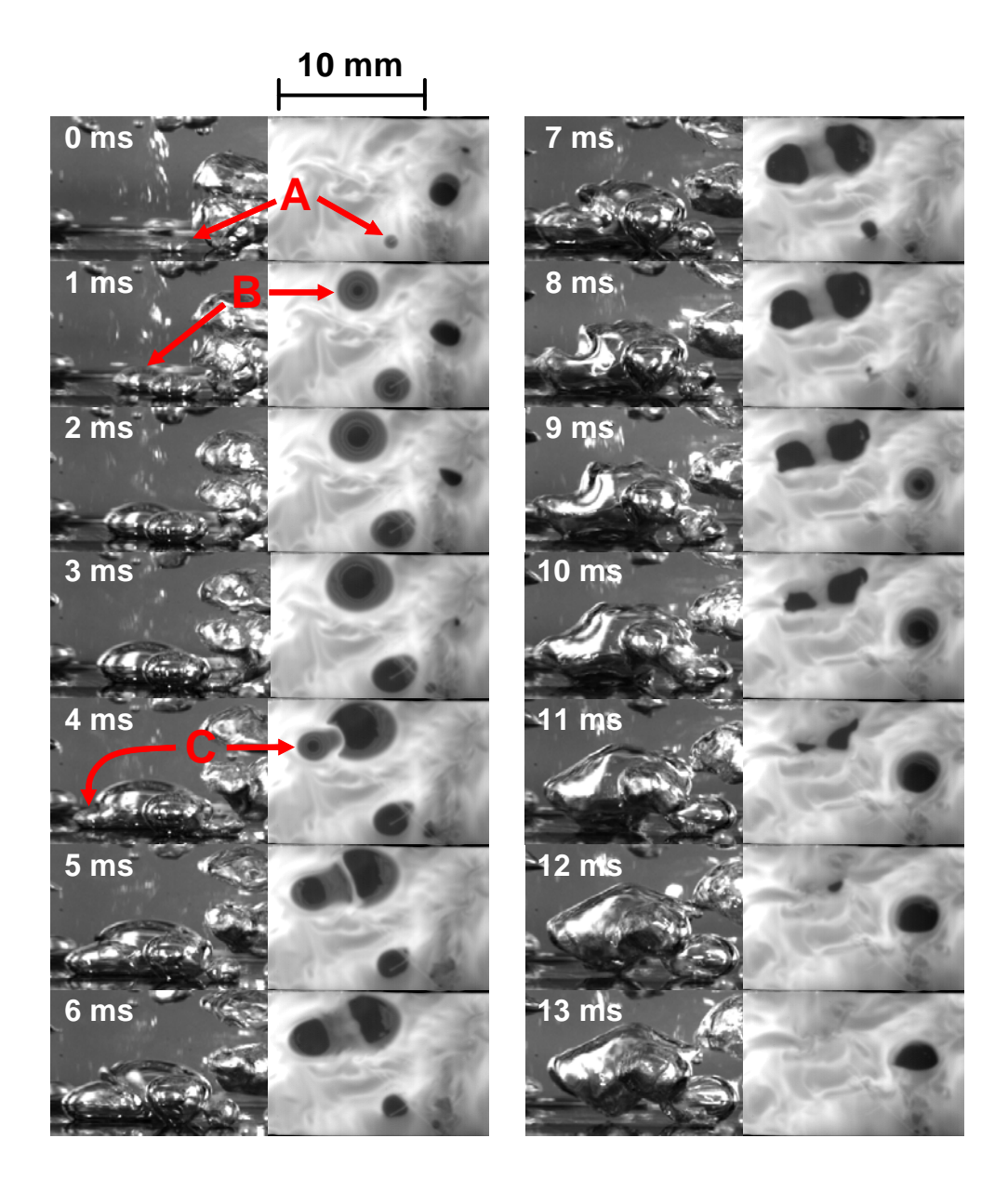


Figure 6. Interactions of bubbles at boiling surface. A, B, and C indicate the bubbles tracked in the synchronized HSV images (lateral view) and IR images (from below the heater).

3.3 Micro-hydrodynamics at high heat flux nucleate boiling, including CHF

It has been recently proposed that nucleate boiling heat transfer at high heat flux is characterized by large dry patches dispersed within an interconnected network of liquid menisci [7]. The geometry of the liquid-vapor-solid triple contact line is highly irregular and dynamic; that is, the liquid menisci advance into and retreat from the dry patches as a function of time, due to the effects of bubble nucleation, liquid inertia (sloshing), capillary forces (surface tension) and recoil forces (evaporation). Theofanous and Dinh [7] refer to this physical situation as the 'microhydrodynamics' of boiling. DEPIcT captures the micro-hydrodynamics very clearly, as shown

in Fig. 7a for boiling of water on the surface of our silicon wafer at ~500 kW/m². Note that large areas of the heater surface appear dry and stay dry for long periods of time (order of 30 ms), though at this heat flux we are still well below CHF, which occurred at ~1100 kW/m² on our silicon wafer heater. In their boiling experiments with ethanol and refrigerants, Nishio and Tanaka [8] and Chung and No [9] also observed large dry areas similar to ours. The wetted area fraction (defined as the ratio of the liquid area to the total surface area) can be obtained by processing of the IR images, and is shown in Fig. 7b; in spite of large instantaneous fluctuations, the wetted area fraction is stable at around 0.49. This is a low value, but obviously sufficient to sustain a very high heat flux without experiencing CHF.

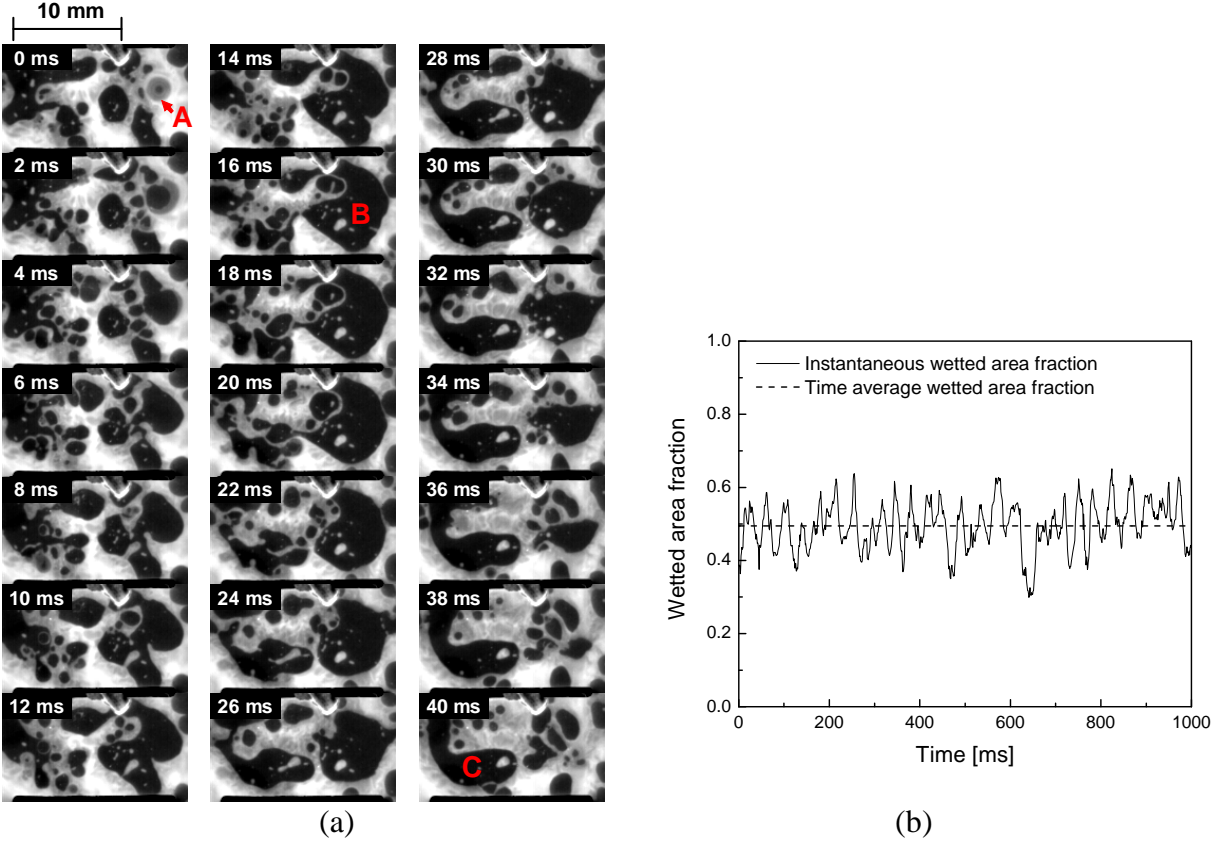


Figure 7. (a) IR images for liquid (bright) and vapor (dark) phase distribution on the wafer heater surface during nucleate boiling of water at high heat flux ($\sim 500 \text{ kW/m}^2$). (b) Time history of wetted area fraction. The images in (a) correspond to time from $\sim 620 \text{ ms}$ to $\sim 660 \text{ ms}$.

The birth mechanism of the dry patches is interesting. For example, a bubble nucleates at point 'A' at 0 ms. The dry spot underneath the bubble rapidly grows due to intense evaporation heat transfer near the liquid-vapor-solid contact line and then merges with the nearby dry spots, forming a larger dry patch, marked as 'B' in the 16-ms image. A large mushroom bubble must be hovering above the dry area, though we could not directly verify this, because the HSV images were too chaotic at such high heat flux. The departure of the mushroom bubble causes the dry patch to shrink gradually, and eventually be rewetted by the incoming flow of the surrounding liquid, as seen between 28 ms and 40 ms. The same life cycles of dry spots/patches are observed over the entire heater surface, for example for the area marked as 'C'. Another

interesting observation is that small liquid fragments, some as big as 1 mm, seem 'trapped' inside the dry patches during the merging process; they are still and survive for relatively long time, $t_{liq}\sim20$ ms. Assuming they receive a heat flux equal to the nominal heat flux, their estimated thickness is at least q $t_{liq}/(\rho_f \, h_{fg})\sim5$ µm, where q is the heat flux, ρ_f is the liquid density and h_{fg} is the heat of evaporation.

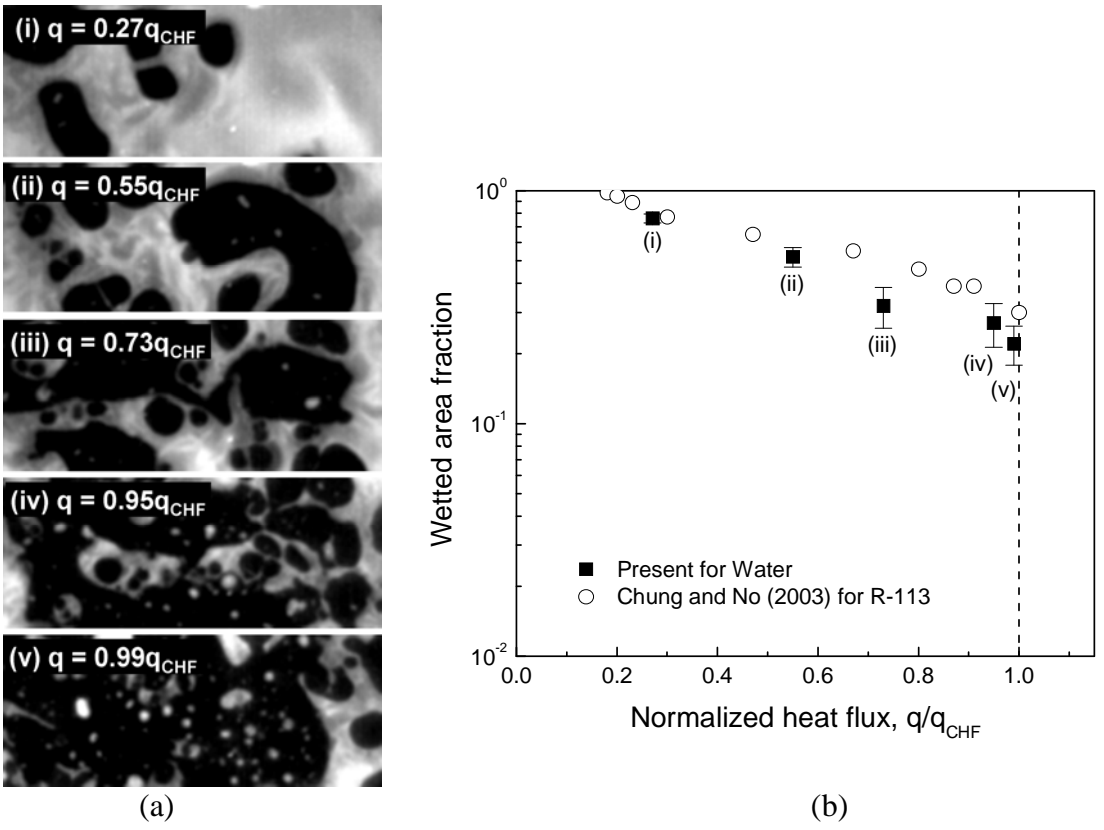


Figure 8. Phase distribution and wetted area fraction at various heat fluxes (normalized to the CHF): (a) IR images of the heater surface; (b) average wetted area fraction.

Similar dynamic behavior of the phases on the wafer surface was observed for other values of the heat flux, all the way up to CHF, as shown in Fig. 8a. The wetted area fraction monotonically decreases with increasing heat flux (Fig. 8b), as expected. At q=0.99q_{CHF} the value of the wetted area fraction is a meager 0.2, yet CHF has not occurred. Note that due to liquid sloshing, no point on the surface is permanently dry; using the IR images we estimated that at q=0.99q_{CHF} the average dry time for any given point on the surface is ~30 ms, with peaks as long as ~60 ms. Then the localized temperature rise of the silicon wafer during a dry period can be estimated as $\Delta T \sim q t_{dry}/(\rho \delta c)$, where t_{dry} is the dry time, and ρ , c and δ are the silicon wafer density, specific heat and thickness, respectively. ΔT ranges from 40 to 70°C. The resulting surface temperatures are well below the Leidenfrost point of the silicon wafer (>200°C), so it makes sense that the liquid can rewet the surface after a dry period. Clearly, little liquid may go a long way in keeping the surface from burning out. The data of Chung and No [9], which are reported for comparison, are similar to ours, in spite of the differences in fluid and heater materials.

DEPicT also allowed us to study CHF itself, i.e., the transition from nucleate boiling to film boiling. Fig. 9 shows that all liquid is basically gone between 4 s and 5 s after the last heat flux step increase. Before CHF occurs, the wetted fraction has large instantaneous fluctuations, but is basically stable at around 0.2. When CHF occurs, the fraction drops to <0.01 in less than a second.

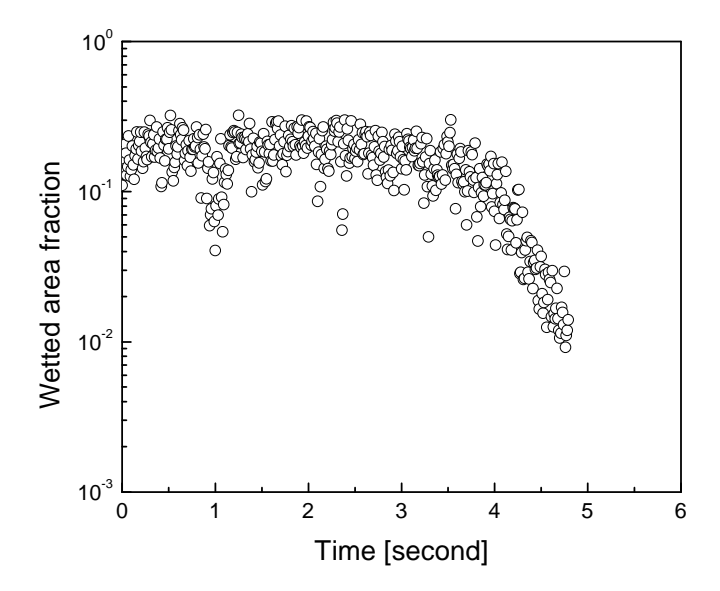


Figure 9. Time history of the wetted area fraction during the transition from nucleate boiling to film boiling ($\sim 1100 \text{ kW/m}^2$).

4. Conclusions

DEPIcT, a new high-speed phase detection technique uniquely suitable for two-phase heat transfer studies, was presented. It is based on IR thermometry through an IR-transparent heater. DEPIcT can detect the liquid-vapor-solid triple line in simple situations such as sliding droplet and single bubble nucleation, but also in more complex situations such as bubble-bubble interaction in nucleate boiling, and CHF. These applications of DEPIcT have generated noteworthy insights, e.g.

- Coalescence of adjacent bubbles in low-heat flux nucleate boiling is *not* accompanied by merging of the bubbles' respective roots. (Confirmation of the mushroom bubble assumption)
- In high heat flux nucleate boiling, the fraction of heater surface area that is well wetted at any given time can be as low as 0.2 without experiencing CHF. However, due to liquid sloshing, no single point on the surface remains dry for more than 30-60 ms, which at a heat flux equal to 99% of the CHF results in a modest temperature rise of 40-70°C, clearly below the rewetting point (Leidenfrost) of silicon.

5. Acknowledgements

This work has been made possible by a Seed Fund grant from the MIT Energy Initiative, and was partially supported by the Korea Science and Engineering Foundation (KOSEF) grant funded by the Korea government (MEST) (No. 2010-0018761). Prof. Karl Berggren and Dr. Sebastian Strobel of MIT are acknowledged for providing the silicon wafers used in this study. Thanks to Dr. Truc-Nam Dinh of the Idaho National Laboratory (INL) for providing useful comments on the work.

6. References

- [1] H. Kim, J. Buongiorno, "Detection of Liquid-Vapor-Solid Triple Contact Line in Two-Phase Heat Transfer Phenomena Using High-Speed Infra-Red Thermometry", Int. J. Multiphase Flow, 37, 166-172, 2011.
- [2] T. G. Theofanous, J. P. Tu, A. T. Dinh and T. N. Dinh, "The Boiling Crisis Phenomenon", J. Experimental Thermal Fluid Science, P.I: pp. 775-792, P.II: pp. 793-810, 26 (6-7), 2002
- [3] E. Wagner and P. Stephan, "High-resolution measurements at nucleate boiling of pure FC-84 and FC-3284 and its binary mixtures", ASME Journal of Heat Transfer, v. 131, n. 12, p. 121008, 2009.
- [4] C. Gerardi, J. Buongiorno, L. W. Hu, T. McKrell, "Study of Bubble Growth in Water Pool Boiling Through Synchronized, Infrared Thermometry and High-Speed Video", Int. J. Heat Mass Transfer, 53, 4185–4192, 2010.
- [5] M. G. Cooper, A. J. P. Lloyd, "The Microlayer in Nucleate Pool Boiling", Int. J. Heat Mass Transfer, 12, pp. 895-913, 1969.
- [6] L. Zhang, M. Shoji, "Nucleation site interaction in pool boiling on the artificial surface", Int. J. Heat Mass Transfer, 46 (3) 513-522, 2003.
- [7] T. G. Theofanous, T. N. Dinh, "High heat flux boiling and burnout as microphysical phenomena: mounting evidence and opportunities", Multiphase Science and Technology 18 (3) 251-276, 2006.
- [8] S. Nishio and H. Tanaka, "Visualization of boiling structures in high-heat flux poolboiling", Int. J. Heat Mass Transfer, 47, 4559-4568, 2004.
- [9] H. J. Chung, H. C. No, "Simultaneous visualization of dry spots and bubbles for pool boiling of R-113 on a horizontal heater", Int. J. Heat Mass Transfer, 46 2239–2251, 2003.